JOURNAL OF PLANKTON RESEARCH | VOLUME 25 | NUMBER 7 | PAGES 855–868 | 2003

Comparisons of *Calanus finmarchicus* fifth copepodite abundance estimates from nets and an optical plankton counter

MARK F. BAUMGARTNER*

COLLEGE OF OCEANIC AND ATMOSPHERIC SCIENCES, OREGON STATE UNIVERSITY, 104 OCEAN ADMINISTRATION BUILDING, CORVALLIS, OR 97331 USA

PRESENT ADDRESS: BIOLOGY DEPARTMENT, WOODS HOLE OCEANOGRAPHIC INSTITUTION, MS #33, WOODS HOLE, MA 02543 USA

*CORRESPONDING AUTHOR: mbaumgartner@whoi.edu

The response of an optical plankton counter (OPC) to concentrations of Calanus finmarchicus fifth copepodites (C5) ranging from 2 to 1621 copepods m^{-3} was examined during the summers of 1999–2001 over the continental shelf of the northwest Atlantic Ocean. Net tows from either a bongo net or a multiple opening/closing net and environmental sensing system (MOCNESS) were collocated with vertical OPC casts to provide comparable data. OPC-derived particle abundance in the 1.5–2.0 mm equivalent circular diameter range was strongly correlated with net-derived abundance of C. finmarchicus C5 (r^2 = 0.655 and 0.726 for comparisons in two independent datasets). Particle abundance in this size range increased with increases in the descent speed of the vertically profiled OPC, which indicated avoidance of the small sampling aperture by C. finmarchicus C5. A regression model was developed to relate OPC particle abundance in the 1.5–2.0 mm size range to the abundance of C. finmarchicus C5 and the descent speed of the OPC. The data fitted the model well (r^2 = 0.684) and the inverted model was used as a calibration equation to predict C. finmarchicus C5 abundances from OPC measurements in an independent comparison to net abundances. In that case, the calibration equation underestimated net abundance by an average factor of 2. However, anomalously low OPC particle abundances for some casts suggest that spatial heterogeneity (patchiness) can confound such comparisons.

INTRODUCTION

The calanoid copepod *Calanus finmarchicus* plays a pivotal trophic role in North Atlantic ecosystems by concentrating phytoplankton and microzooplankton biomass and making it directly available to higher trophic levels, such as fish, birds and some marine mammals. *Calanus finmarchicus* has garnered much attention in recent years (Tande and Miller, 1996; Wiebe *et al.*, 2001) because its life history and population dynamics have a significant impact on so many other species. One such species is the North Atlantic right whale (*Eubalaena glacialis*). This highly endangered baleen whale feeds primarily on older copepodite stages of *C. finmarchicus* in its summer feeding grounds over the continental shelf of the northwestern Atlantic Ocean (Stone *et al.*, 1988; Murison and Gaskin, 1989; Woodley and Gaskin, 1996). By summer, *C. finmarchicus* has already undertaken its ontogenetic downward migration and the population is primarily in the resting, fifth copepodite (C5) stage at depth (Miller *et al.*, 1991; Hirche, 1996). To understand better important aspects of right whale ecology, particularly its foraging behaviour and habitat, a method was required to rapidly assess the horizontal and vertical distribution and abundance of *C. finmarchicus* C5. The optical plankton counter (OPC) (Herman, 1988, 1992) has been used as just such a rapid assessment tool in several applications (Sameoto and Herman, 1990; Herman *et al.*, 1991; Heath, 1995; Huntley *et al.*, 1995; Stockwell and Sprules, 1995; Checkley *et al.*, 1997; Osgood and Checkley, 1997). The performance of the OPC has been examined in a wide variety of environments (Herman *et al.*, 1993; Sameoto *et al.*, 1993; Wieland *et al.*, 1997; Sprules *et al.*, 1998; Grant *et al.*, 2000; Woodd-Walker *et al.*, 2000; Zhang *et al.*, 2000; Halliday *et al.*, 2001), and it has shown promise in estimating the abundance of older stages of *Calanus* spp. (Osgood and Checkley, 1997; Heath *et al.*, 1999).

The OPC consists of a light source and a detector

housed in the middle of a flow tunnel through which water passes (Herman, 1988, 1992). Particles in the water partially occlude the collimated beam formed by the light source as they pass through the tunnel. The magnitude of the occlusion measured at the detector is related to the illuminated cross-sectional area of the particle. The OPC, therefore, provides an estimate of numbers and sizes of particles passing through the tunnel. The challenges of making sensible measurements with the OPC are similar to those faced by other rapid assessment methods. Both the OPC and video methods [e.g. (Davis *et al.*, 1992, 1996)] sample relatively small volumes. In a patchy environment, significant concentrations of zooplankton may not be sampled by the instrument, so abundance may be underestimated. Statistical power is also reduced when estimating the concentration of less abundant mesozooplankton from small sample volumes. Furthermore, the small aperture through which particles pass to be sampled by these instruments is susceptible to avoidance by zooplankton. Unlike high-quality video, the OPC and acoustic methods (Holliday and Pieper, 1995) are hampered by their lack of taxonomic discrimination. In particular, a major constituent of OPC-observed particles in neritic waters is thought to be detrital material (Herman, 1992), which may impede taxonomic discrimination based on particle size alone. At high particle concentrations, the OPC is also prone to coincident counts, a phenomenon that occurs when two or more particles occlude the light beam simultaneously and are recorded as a single, larger particle (Herman, 1988; Sprules *et al.*, 1998).

Despite these challenges, the zooplankton community near feeding right whales has characteristics ideal for applying the OPC. The average water column abundance of *C. finmarchicus* C5 is typically in the upper hundreds to low thousands of copepods m^{-3} (Murison and Gaskin, 1989; Mayo and Marx, 1990; Wishner *et al.*, 1995; Woodley and Gaskin, 1996) and the abundances at depth, where the whales concentrate their feeding, are probably much higher (Kenney *et al.*, 1986). Statistical power, therefore, should not be a problem. *Calanus finmarchicus* C5 is typically the dominant zooplankter of its size near right whales, so discrimination based on size alone seems possible. Detrital material, however, is ubiquitous over the continental shelves, so size discrimination may be difficult. In fact, Heath and colleagues (Heath *et al.*, 1999) suggest that 'the high incidence of detrital aggregates would seem to preclude the use of the OPC [for measuring late-stage *C. finmarchicus*] in continental shelf waters'. They based this conclusion on poor correlations between OPC-derived particle abundances and net-derived abundances of *C. finmarchicus* C4 and C5 between 0.05 and 500 copepods m^{-3} in the upper 200 m of the Faroe–Shetland Channel.

This paper examines the response of the OPC to *C. finmarchicus* C5 abundances between 2 and 1621 copepods m^{-3} in a neritic environment. OPC particle abundances were compared to net-derived abundance estimates to determine in which particle size range *C. finmarchicus* C5 could be detected. Avoidance of the OPC's small tunnel opening (2 × 25 cm) by *C. finmarchicus* C5 was also investigated by changing the descent speed for some OPC casts that accompanied net tows. A separate dataset consisting of paired OPC casts in which the descent speed was either varied or held constant between two successive casts was also used to examine avoidance by *C. finmarchicus* C5. Finally, a model relating OPC particle abundance and *C. finmarchicus* C5 abundance was developed and tested with independent data for comparison with the results of Heath and colleagues (Heath *et al.*, 1999). The inverted model is intended to be used as a calibration equation to estimate the abundance of *C. finmarchicus* C5 from OPC-derived particle abundance in future studies.

METHOD

A Focal Technologies OPC (model OPC-1T) was mounted in the centre of an open, 0.8 m diameter by 1.0 m height, cylindrical, galvanized steel cage such that the downward-facing tunnel opening was 2–3 cm from the bottom of the cage. Two different instruments were used in this study: serial numbers TOW015 in 1999 and TOW047 in 2000 and 2001. A conductivity–temperature–depth (CTD) instrument was also housed in the cage. Flow into and around the OPC was unobstructed. During 2000 and 2001, depth was measured by a pressure sensor in the OPC. The OPC was not equipped with a flowmeter, so the volume of water passing through the instrument was estimated simply as the product of the tunnel opening area (0.005 m^2) and the depth traversed by the OPC when profiled vertically. When a cast was not exactly vertical, the calculated volume is an underestimate of the true sampled volume and the resulting particle abundance is overestimated. The per cent error in the calculated volume for wire angles (θ) relative to the vertical is $100[\cos(\theta)-1]$ and is less than 10, 20 and 30% for angles as great as 25°, 36° and 45°, respectively. Wire angles during casts were not explicitly measured, but were typically <30°. The OPC was always deployed in a vertical cast and only the data from the downcast were used. Automated post-processing of the casts removed data associated with (i) low descent speeds (<0.3 m s^{-1}), (ii) direction reversals (during periods of high swell), (iii) excessive changes in relative light attenuance, (iv) non-sequential timer values and (v) invalid timer, depth, or relative light attenuance values. The instrument calibration was checked before and after the 2001 field season

by passing 1.59, 2.38 and 3.18 mm diameter nylon beads through the OPC (corresponding to average digital values of 228, 455 and 749, respectively). Measurement errors were within the manufacturer's specifications of 10% accuracy error (Focal Technologies, 1999). Particle sizes are expressed in units of equivalent circular diameter (ECD), which is the diameter of a circle that has the same area as the illuminated cross-section of the particle.

Collocated net and OPC sampling

Zooplankton samples were collected with 61 cm bongos equipped with 333 μm mesh nets. A CTD was affixed to the tow wire ~1 m above the bongo to telemeter the depth of the nets to the ship. The bongo was lowered at 0.50 m s^{-1} to within 5–10 m of the bottom and then hauled in at 0.33 m s^{-1}. The ship steamed at 0.8–1.0 m s^{-1} (1.5–2.0 knots) during tows. A flowmeter was mounted in the centre of each bongo to estimate the volume filtered by the nets. Depth-stratified, 1 m^2 multiple opening/closing net and environmental sensing system (MOCNESS) (Wiebe *et al.*, 1976, 1985) tows were conducted during 2001 in lieu of bongo tows. The MOCNESS was equipped with six, 150 μm mesh nets and the first of these remained open during the entire downcast to within 10 m of the bottom. The remaining five nets were towed through contiguous depth strata from the bottom of the downcast to the surface. The MOCNESS was towed at 0.5–1.0 m s^{-1} (1.0–2.0 knots) and paid out and hauled in at 0.33 m s^{-1}. The volume filtered by the nets was estimated from a flowmeter positioned outside the net mouth. Zooplankton samples were preserved in a 5% borate-buffered formalin and seawater solution and were subsampled in the laboratory with a Hensen stempel pipette. Subsample volumes were obtained such that 100 or more of the most abundant copepod species were counted. *Calanus finmarchicus* copepodite stages C3 and higher were counted separately while all other taxa were identified to species or genus level. More than 100 *C. finmarchicus* C5 were counted in 74% of the samples (52 of 70) and for those cases where fewer than 100 were counted, the *C. finmarchicus* C5 abundance was typically <55 copepods m^{-3} (14 of 18 cases) and always <200 copepods m^{-3}.

Each bongo tow was collocated with a single OPC cast that was usually conducted immediately prior to the net sampling. A total of 26 collocated bongo tows and OPC casts were conducted on the central and southwestern Scotian Shelf (n = 12) and in the lower Bay of Fundy (n = 14) aboard NOAA Ship *Delaware II* (cruise DE9908) from July 26 to September 3, 1999 (Figure 1; Table I). Fourteen bongo tows with accompanying OPC casts were conducted in the lower Bay of Fundy (n = 11) and on the southwestern Scotian Shelf (n = 3) from July 7 to August 31, 2000 aboard NOAA Ship *Delaware II* (cruise DE0007).

From July 23 to August 3, 2001, six MOCNESS tows were conducted from NOAA Ship *Albatross IV* (cruise AL0108) in the lower Bay of Fundy (Figure 1; Table I). These tows were conducted at slack tide and collocated with four OPC casts to reduce differences between the net and OPC abundance estimates attributable to advection of *C. finmarchicus* C5 and horizontal variability in copepod distribution. The local time of slack tide was predicted by TIDES & CURRENTS software (version 2.0) (Nautical Software, 1996) based on US National Oceanic and Atmospheric Administration and Canadian Hydrographic Service harmonic constants. The MOCNESS was towed through a station immediately after two OPC casts were completed there. After the tow, two more OPC casts were conducted at the midpoint of the tow. To investigate the effect of copepod avoidance (see below), three of the MOCNESS tows were accompanied by OPC casts conducted at a nominal descent speed of just over 0.5 m s^{-1} (referred to as the 'slow' AL0108 data). The remaining three MOCNESS tows were accompanied by OPC casts conducted at a nominal descent speed of just below 1.0 m s^{-1} (referred to as the 'fast' AL0108 data).

OPC-derived particle abundances were computed only

Table I: Collocated net and OPC deployment information for each cruise

Cruise	Sampling equipment	Tow type	Mesh size (μm)	No. of tows	No. of samples	OPC casts per tow	OPC descent speed range (m s^{-1})
DE9908	Bongo	double oblique	333	26	26	1	0.44–0.56
DE0007	Bongo	double oblique	333	14	14	1	0.60–0.92
AL0108[a]	MOCNESS	depth stratified	150	3	15	4	0.59–0.66
AL0108[b]	MOCNESS	depth stratified	150	3	15	4	0.87–0.98

[a]Referred to in the text as the 'slow' AL0108 data.
[b]Referred to in the text as the 'fast' AL0108 data.

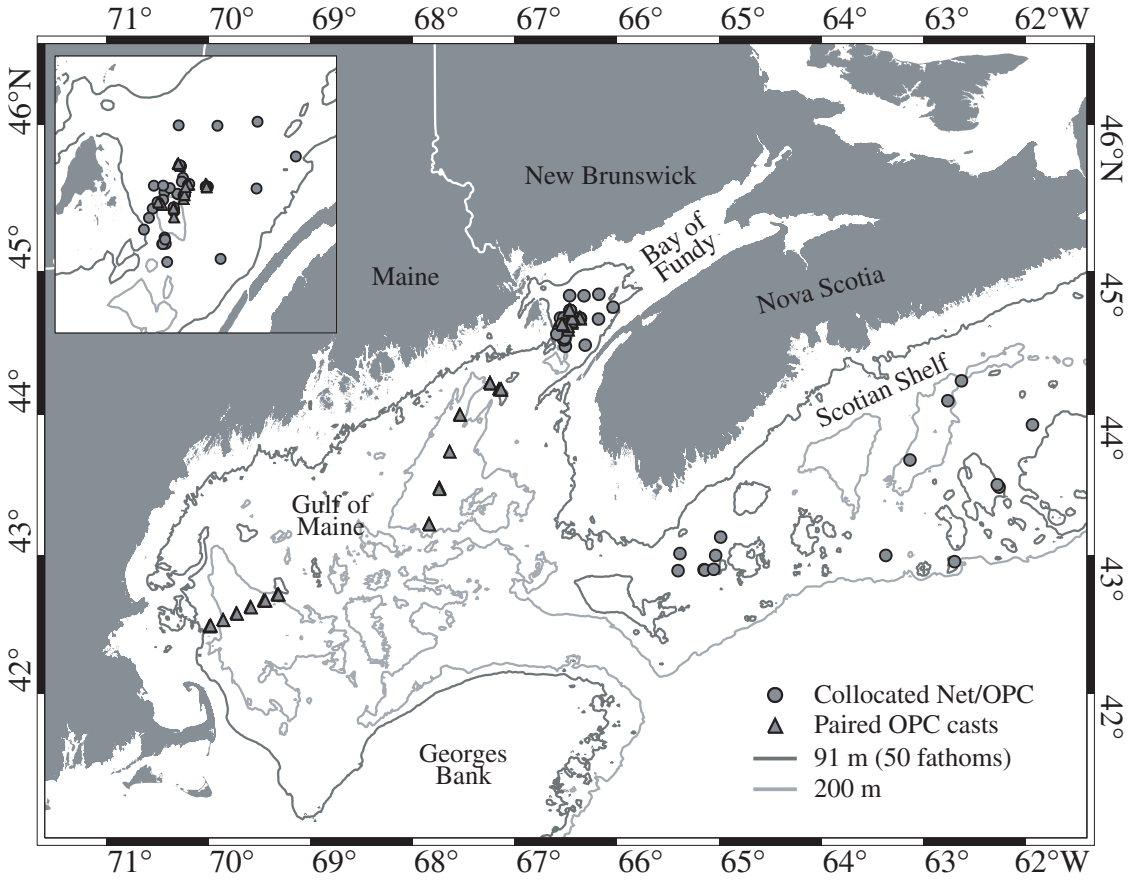

Fig. 1. Study area and locations of collocated OPC casts and net tows (filled circles) and paired OPC casts (filled triangles). Inset shows the study area in the lower Bay of Fundy. The 91 m (50 fathom) and 200 m isobaths are shown.

over the depths that were sampled during the bongo and MOCNESS tows to provide comparable data. The particle abundances from the four OPC casts accompanying each MOCNESS tow were averaged to obtain a single particle abundance estimate for each MOCNESS net sample.

Optimum size range detection

The size range in which *C. finmarchicus* C5 could be best detected was determined using similar methods to those employed by Heath and colleagues (Heath *et al.*, 1999). Particle abundances were computed from the OPC data over a matrix of size ranges systematically defined by the minimum and span of the size range [equivalently, the mid-point and the span of the size range were used in (Heath *et al.*, 1999)]. The minimum of the size range in the matrix varied from 0.25 to 3 mm in 0.05 mm increments and the span of the size range in the matrix varied from 0.20 to 2 mm in 0.05 mm increments. A regression procedure was first used to measure the strength of linear association between the log-transformed, OPC-derived particle abundances and the collocated, log-transformed, net-derived abundances of *C. finmarchicus* C5 in each of the size ranges of the matrix. The regression coefficients ($a_{i,j}$ and $b_{i,j}$) and the coefficient of determination ($r_{i,j}^2$) were estimated for the following model

$$\log_{10}(OPC) = a_{i,j} + b_{i,j} \log_{10}(NET) \quad (1)$$

where *OPC* is the particle abundance in the size range indexed by i and j in the matrix (i.e. with a minimum size indexed by i and a span of the size range indexed by j) and *NET* is the net-derived *C. finmarchicus* C5 abundance. Cases where the OPC-derived particle abundance was 0 particles m^{-3} were excluded from the model, and the regression was only performed when 50% or more of the cases had particle abundances >0 particles m^{-3}. The regression procedure was conducted on data from a single cruise only. Data from a second cruise were used in a validation procedure to assess independently the predictive capabilities of the equations obtained in the regression

procedure. Predicted abundances of *C. finmarchicus* C5 were computed from the OPC particle abundances in the validation dataset by inverting equation (1). A root mean square error (RMSE) for the predicted net abundances was computed as follows

$$RMSE_{i,j} = \sqrt{\langle 1/n \sum_{k=1}^{n} \{[\log_{10}(OPC_k) - a_{i,j}/b_{i,j}] - \log_{10}(NET_k)\}^2\rangle} \quad (2)$$

where $a_{i,j}$ and $b_{i,j}$ are the coefficients obtained in the regression procedure (equation 1), *OPC* and *NET* are the particle and *C. finmarchicus* C5 abundances, respectively, and n is the number of cases in the validation dataset. The RMSE was only computed when at least 50% of the validation cases had OPC-derived particle abundances >0 particles m^{-3} (cases with particle abundances of 0 particles m^{-3} were excluded from the validation procedure). *Calanus finmarchicus* C5 was considered to be best detected in those size ranges in which (i) the linear association between the particle abundance and the net-derived C5 abundance was strong (high $r_{i,j}^2$) and (ii) the predictive capability of the detected linear relationship when applied to independent data collected in other years and at different locations was high (low $RMSE_{i,j}$). Based on these criteria, a single size range was selected for further analysis and is referred to as the optimum size range.

The OPC and net data from DE9908 (n = 26) were used in the regression procedure, and the OPC data from the 'slow' casts during AL0108 and the corresponding MOCNESS net data (n = 15) were used in the validation procedure. Since the assignment of these datasets to the regression or validation procedures is arbitrary, a second analysis of the optimum size range was conducted with the 'slow' AL0108 data and the DE9908 data assigned to the regression and validation procedures, respectively. The DE9908 and 'slow' AL0108 data were chosen for these analyses because the descent speeds of the OPC casts do not vary much within each cruise and are nearly comparable between the two cruises (Table I).

Avoidance: multiple linear regression analysis

To examine avoidance of the OPC by *C. finmarchicus* C5, the effect of descent speed on particle abundance in the optimum size range was tested using multiple linear regression analysis. Avoidance is expected to decrease as descent speed increases because the time for a copepod to react to the oncoming instrument decreases as the descent speed increases (Barkley, 1972). Therefore, measured particle abundance was expected to increase with increasing descent speed if avoidance occurs. The AL0108 MOCNESS tows were accompanied by OPC casts of different descent speeds to test this hypothesis (Table I) and these data were used in the multiple linear regression analysis. The particle abundance in the optimum size range (*OPC*) was regressed against both the MOCNESS-derived abundance of *C. finmarchicus* C5 (*NET*) and the descent speed (*SPEED*) in the following model

$$\log_{10}(OPC) = \beta_0 + \beta_1 \log_{10}(NET) + \beta_2 SPEED \quad (3)$$

If significant, the back-transformed regression coefficient for the descent speed (10^{β_2}) indicates the multiplicative change in the median particle abundance corresponding to a 1 m s^{-1} increase in the descent speed after accounting for the effect of the net-derived abundance of *C. finmarchicus* C5 on the particle abundance (Ramsey and Schafer, 1997). The base 10 logarithm of the multiplicative change in the median particle abundance for any increase in descent speed from $SPEED_{slow}$ to $SPEED_{fast}$ can then be expressed as

$$\log_{10}(OPC_{fast}/OPC_{slow}) = \beta_2(SPEED_{fast} - SPEED_{slow}) \quad (4)$$

Avoidance: paired OPC casts

OPC casts were also conducted in rapid succession at the same station (paired OPC casts) to investigate further the effect of descent speed on particle abundance. The descent speeds for the two casts were either held constant (<0.1 m s^{-1} difference between the two) or deliberately varied (>0.3 m s^{-1} difference). The average water column particle abundance in the optimum size range was computed for each cast over the common depths sampled in both casts. The log-transformed ratio of these particle abundances was then regressed against the difference in descent speeds between the two casts using the following equation

$$\log_{10}(OPC_{fast}/OPC_{slow}) = \alpha(SPEED_{fast} - SPEED_{slow}) \quad (5)$$

where *OPC* is the particle abundance, *SPEED* is the descent speed, α is the slope of the regression line forced through the origin and the indices 'fast' and 'slow' indicate the cast in the pair with the faster or slower descent speed, respectively. The back-transformed slope of the regression line (10^{α}) provides an estimate of the multiplicative change in the median particle abundance corresponding to a 1 m s^{-1} increase in the descent speed and is directly comparable to the coefficient β_2 in equations (3) and (4).

Paired OPC casts with varying descent speeds were conducted in Wilkinson and Jordan Basins in the Gulf of Maine during cruise AL0108 (n = 9) and during another cruise conducted aboard NOAA Ship *Delaware II* (cruise DE0108) from August 7 to August 31, 2001 (n = 10) (Figure 1). Paired OPC casts with nearly constant descent

speeds were conducted in the Gulf of Maine during DE9908 (n = 8) and in the lower Bay of Fundy during AL0108 (n = 12). The latter paired OPC casts were the same casts conducted before and after each MOCNESS tow during AL0108.

Final model development

A final regression model of the form in equation (3) was developed as the 'best fit' between the OPC data and the net-derived *C. finmarchicus* C5 abundance. This model was fitted using the DE9908 and all AL0108 data and inverted to produce the following calibration equation

$$\log_{10}(C5) = (1/\beta_1)[\log_{10}(OPC) - \beta_0 - \beta_2 SPEED] \quad (6)$$

where $C5$ is the abundance of *C. finmarchicus* C5 in copepods m^{-3}. Since the descent speeds of the DE0007 data varied much more than in any of the other datasets (Table I), these data were excluded from the final model development and were used to assess independently the prediction errors in the calibration equation. One case was removed from the DE0007 data prior to this assessment because the OPC-derived particle abundance in the optimum size range was 0 particles m^{-3} (the corresponding net abundance for *C. finmarchicus* C5 was 29.0 copepods m^{-3}).

Caveats

All of the comparisons described above assume that the population of copepods remains the same during collocated sampling so that the performance of the OPC can be directly evaluated. Violations of this assumption are caused by spatial heterogeneity in copepod distribution (patchiness) interacting with advection, ship drift or an incompatibility in the spatial scales over which different methods sample. When the assumption is not met, variability will occur in the comparisons, and serious violations will cause outliers. This variability is independent of the OPC's performance and is the consequence of a genuine feature of copepod distribution in the ocean and the sampling methodology employed here. Truly collocated sampling (e.g. mounting an OPC on a net system) may reduce the effect of copepod patchiness on the comparisons, but the intent of this study was to assess the performance of the OPC under the same deployment conditions that were used in concurrent studies of right whales and *C. finmarchicus* C5 (i.e. a vertical cast with no accompanying net sampler).

RESULTS

Optimum size range detection

The average particle size distribution in regions of high *C. finmarchicus* C5 abundance was characterized by a modal peak at ~1.55 mm (Figure 2a). This mode was absent in regions of lower *C. finmarchicus* C5 abundance. At intermediate abundances, the modal distribution is obscured by smaller particles. Herman and Edvardsen (Herman, 1992; Edvardsen, 2002) measured the response

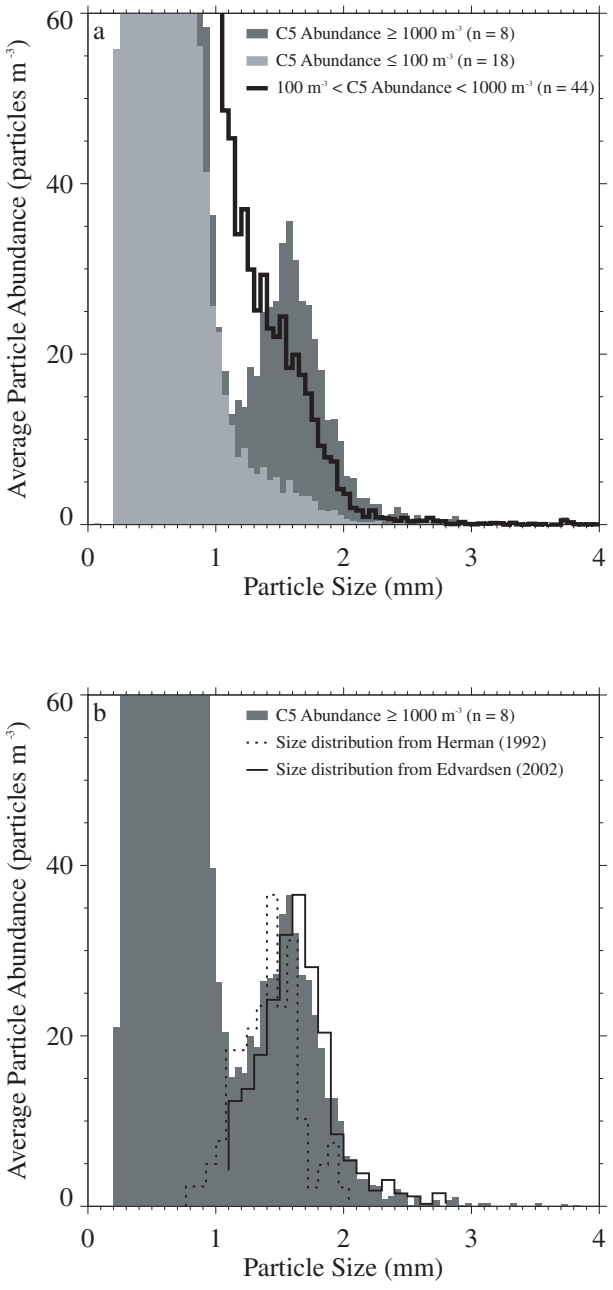

Fig. 2. (**a**) Average particle size distributions (in units of equivalent circular diameter) for OPC casts associated with tows that yielded *Calanus finmarchicus* C5 abundances in excess of 1000 copepods m^{-3} (dark grey), less than 100 copepods m^{-3} (light grey) and between 100 and 1000 copepods m^{-3} (thick line). (**b**) Comparison of average OPC response at high *C. finmarchicus* C5 abundance (dark grey) with comparably scaled laboratory-derived distributions of preserved (Herman, 1992) (dotted) and live (Edvardsen, 2002) (solid line) *C. finmarchicus* C5.

of the OPC to preserved and live *C. finmarchicus* C5, respectively, in the laboratory (Figure 2b). A similar modal peak to the one observed at high *C. finmarchicus* C5 abundance in the field is apparent in each of these laboratory-derived size distributions. The apparent 0.1–0.2 mm offset in modes is likely to be attributable to calibration differences, preservation effects (e.g. shrinkage, increase in opacity) or true differences in size distributions. Despite these effects, the field- and laboratory-derived distributions are in good agreement.

The regression procedure on the DE9908 data indicated a peak in the coefficient of determination over the size range defined by a minimum of 1.90 mm and a span of 0.95 mm (r^2 = 0.784; Figure 3a). A similar result was obtained in the regression procedure on the 'slow' AL0108 data, however the peak in the coefficient of determination occurred at a minimum size of 1.75 mm and a span of 0.40 mm (r^2 = 0.843). A local maximum occurred in both analyses at a minimum size of 1.5 mm, although this feature is more pronounced in the DE9908 data (Figure 3a). When the validation procedure was applied to the independent data, a single minimum was observed in the root mean square error for both analyses at a minimum particle size of 1.5 mm (Figure 3b). These

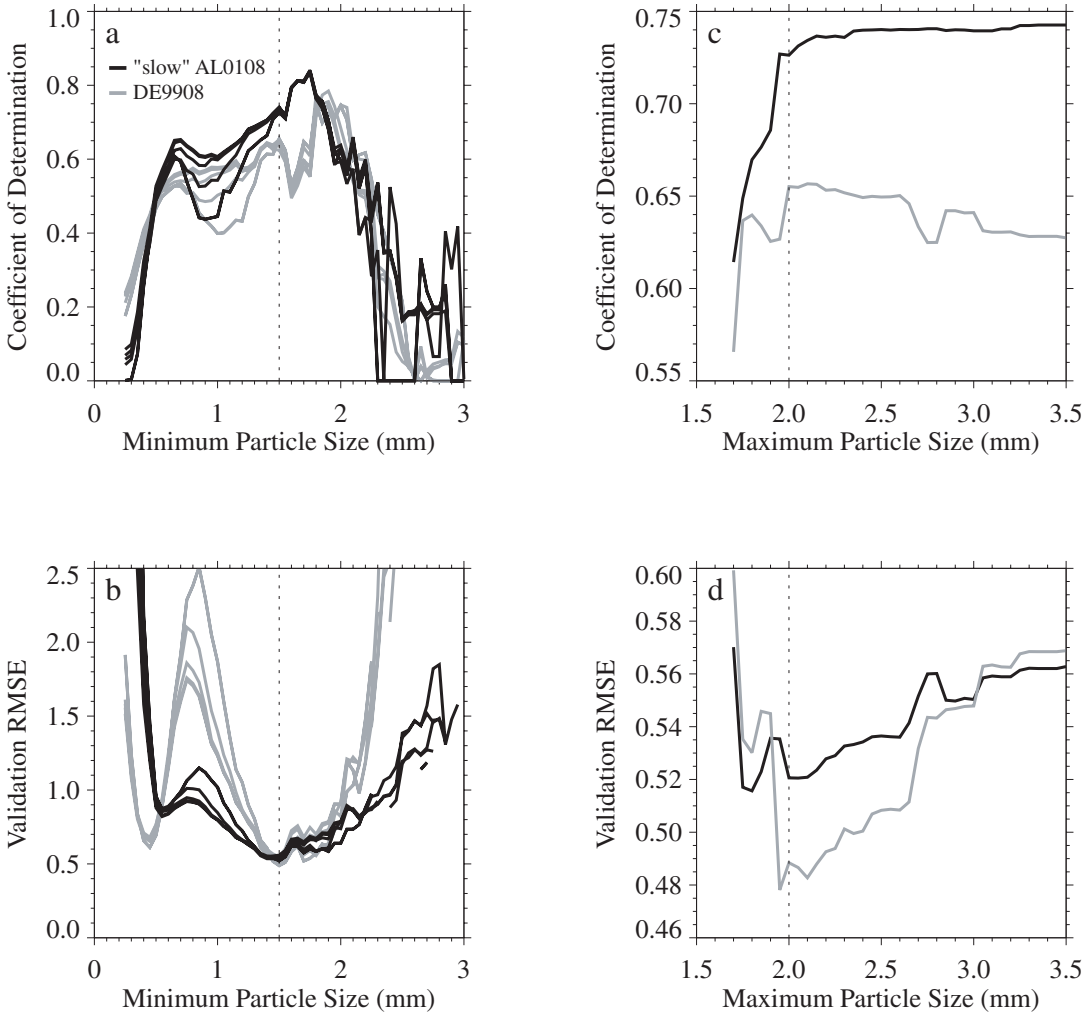

Fig. 3. (**a**) Coefficients of determination (r^2) obtained in the regression procedure on the DE9908 (grey) and 'slow' AL0108 (black) data for all minimum particle sizes and spans of 0.50, 0.75, 1.00, 1.25 and 1.50 mm. The spans are not differentiated because r^2 is primarily a function of minimum size. (**b**) Root mean square errors (RMSE) obtained by applying the DE9908 (grey) and 'slow' AL0108 (black) regressions to the validation datasets for all minimum particle sizes and the same spans as in (**a**). (**c**) r^2 obtained in the regression procedure on the DE9908 (grey) and 'slow' AL0108 (black) data for all maximum particle sizes associated with a minimum size of 1.5 mm. The maximum size is simply the sum of the minimum size and the span. (**d**) RMSE obtained by applying the DE9908 (grey) and 'slow' AL0108 (black) regressions to the validation datasets for all maximum particle sizes associated with a minimum size of 1.5 mm. The dotted line indicates the minimum of the optimum particle size range (1.5 mm) in (**a**) and (**b**) and the maximum of the optimum particle size range (2.0 mm) in (**c**) and (**d**).

results suggest that better correlation can be achieved between OPC particle abundance and net-derived C5 abundance at minimum sizes above 1.5 mm, but the best agreement between the regression equations and the independent data occurs in size ranges with a minimum of 1.5 mm. For both datasets, the coefficient of determination reaches an asymptote for the size range that has a minimum value of 1.5 mm and a maximum value of 2.0 mm (a span of 0.5 mm; Figure 3c) while the RMSE reaches a minimum near this same size range (Figure 3d). An analysis of covariance (Zar, 1999) provided no evidence to suggest that the slopes ($P = 0.26$), elevations ($P = 0.47$) or overall regressions ($P = 0.40$) in the 1.5–2.0 mm size range were different in the two datasets (Figure 4). Based on these results, the 1.5–2.0 mm size range is considered the optimum size range.

Avoidance: multiple linear regression analysis

There was strong evidence that the particle abundance observed by the OPC in the optimum size range during AL0108 increased with increasing descent speed after accounting for the net-derived abundance of *C. finmarchicus* C5 ($P = 0.0009$; Table II). The coefficient for the descent speed in the multiple linear regression model (β_2 in equations 3 and 4) was 1.21 s m^{-1} (95% CI: 0.541–1.88 s m^{-1}).

Avoidance: paired OPC casts

There was also strong evidence that an increase in particle abundance was associated with an increase in the descent speed during the paired OPC casts ($P = 0.0002$; Figure 5). Before fitting the model in equation (5), an intercept was included to test for a change in particle abundance when the descent speed was held constant, but this term was not found to be significant ($P = 0.11$). Note that two sets of paired OPC casts were excluded from the regression analysis because the ratios of the particle abundances were considered outliers (Figure 5). Each of these sets of casts was conducted near a right whale, an area where *C. finmarchicus* C5 abundance is typically patchy (Wishner *et al.*, 1988, 1995; Mayo and Marx, 1990; Beardsley *et al.*, 1996). I suspect that the two casts in each of the sets were not sampling the same population of copepods (i.e. one was in a patch upon which the right whale was probably feeding and the other was outside of the patch). The slope of the regression forced through the origin (α in equation 5) was 0.412 s m^{-1} (95% CI: 0.210–0.615 s m^{-1}), which was significantly lower than the comparable estimate of 1.21 s m^{-1} obtained in the multiple linear regression analysis ($P < 0.0001$).

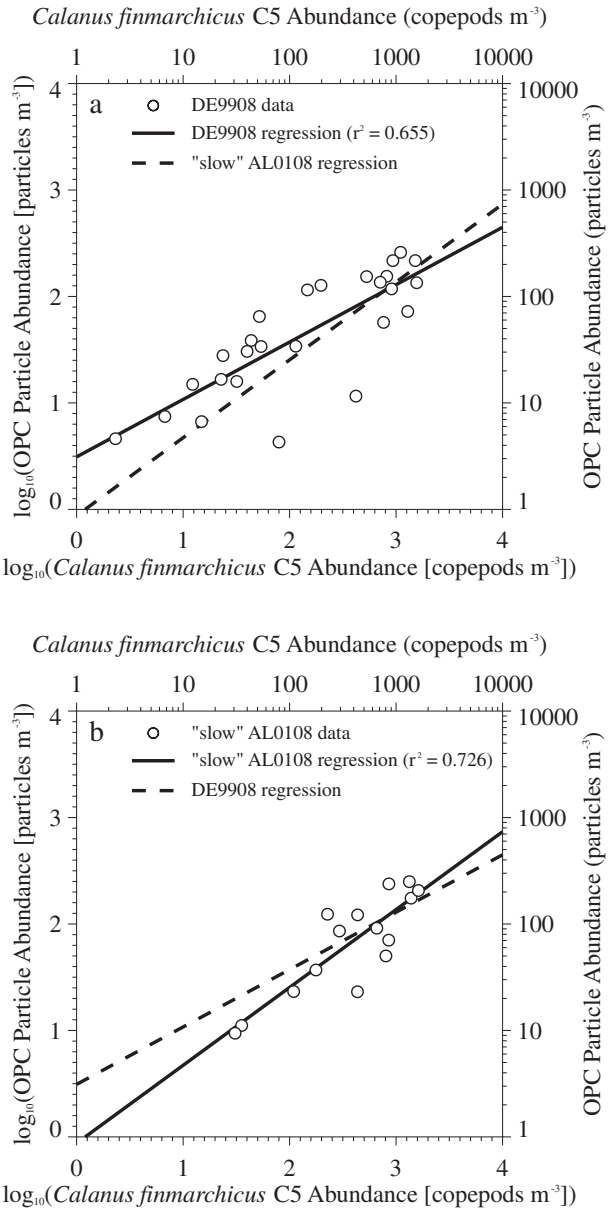

Fig. 4. (**a**) Scatterplot of log-transformed *C. finmarchicus* C5 abundance and OPC particle abundance in the optimum size range of 1.5 to 2.0 mm for the DE9908 data (circles). The regression line is shown as a solid line and the independent regression of the 'slow' AL0108 data for which the DE9908 data serve as the validation dataset is shown as a dashed line. (**b**) Similar scatterplot of 'slow' AL0108 data (circles) with regression line (solid line). The independent regression of the DE9908 data for which the 'slow' AL0108 data serve as the validation dataset is shown as a dashed line.

Final model development

The final regression model fitted the DE9908 and AL0108 data well ($r^2 = 0.684$) and was highly significant ($P < 0.0001$) (Table III; Figure 6). When applied to the

Table II: Multiple linear regression analysis to investigate avoidance of the OPC by Calanus finmarchicus C5

Variable	Coefficient	Estimate	Standard error	95% CI	*t* statistic	*P* value
Intercept	β_0	–0.5865	0.3749	–1.3558–0.1829	–1.56	0.1294
$\log_{10}$(NET)	β_1	0.6310	0.1193	0.3861–0.8758	5.29	< 0.0001
SPEED	β_2	1.2101	0.3260	0.5412–1.8789	3.71	0.0009

All AL0108 data were fitted to equation (3) to test for the effect of descent speed on OPC-derived particle abundance in the 1.5–2.0 mm size range (n = 30, r^2 = 0.645, F = 24.55, P < 0.0001).

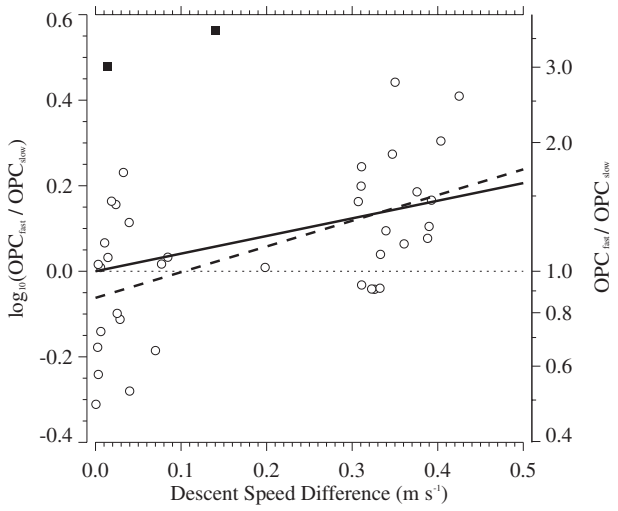

Fig. 5. Scatterplot of descent speed difference and the ratio of OPC particle abundance in the optimum size range for paired OPC casts. The regression line forced through the origin (see equation 5 in the text) is shown as a solid line and the regression line with both a slope and intercept is shown as a dashed line. The regressions excluded the two observations with anomalously high ratios at low descent speed differences (filled squares).

DE0007 data using equation (6) (Figure 7), however, there was suggestive, but inconclusive, evidence that the mean prediction was different from the actual *C. finmarchicus* C5 abundance (P = 0.060). The predicted *C. finmarchicus* C5 net abundance was underestimated by an average factor of 1.95 [95% CI: 3.91 (too low) to 1.03 (too high)].

DISCUSSION

The modal peak in the average size distribution at 1.55 mm is unambiguous at high concentrations of *C. finmarchicus* C5, but is absent at lower concentrations (Figure 2a). Furthermore, the regression and validation procedures suggest that the OPC-observed particles in the size range 1.5–2.0 mm are *C. finmarchicus* C5. These results indicate that *in situ C. finmarchicus* C5 is best detected by the OPC in only the larger half of its laboratory-derived size distribution (Herman, 1992; Edvardsen, 2002) where its abundance is not obscured by other, smaller particles. The total abundance of smaller copepods (e.g. *C. finmarchicus* C3 or C4, *Centropages* spp., *Pseudocalanus* spp., *Metridia lucens*, *Temora longicornis* and *Acartia longiremis*) exceeded that of *C. finmarchicus* C5 in nearly 50% of the net samples, whereas the total abundance of larger copepods (e.g. *C. finmarchicus* adults, *Metridia longa*, *C. glacialis*, *C. hyperboreus*)

Table III: Final multiple linear regression model

Variable	Coefficient	Estimate	Standard error	95% CI	*t* statistic	*P* value
Intercept	β_0	0.0384	0.1825	–0.3276–0.4044	0.21	0.8341
$\log_{10}$(NET)	β_1	0.5343	0.0626	0.4087–0.6598	8.53	< 0.0001
SPEED	β_2	0.8001	0.2370	0.3248–1.2754	3.38	0.0014

Model fit to all AL0108 and DE9908 data (n = 56, r^2 = 0.684, F = 57.32, P < 0.0001).
Coefficients from this model can be used in equation (6) to predict *C. finmarchicus* C5 abundance from OPC-derived particle abundance in the 1.5–2.0 mm size range.

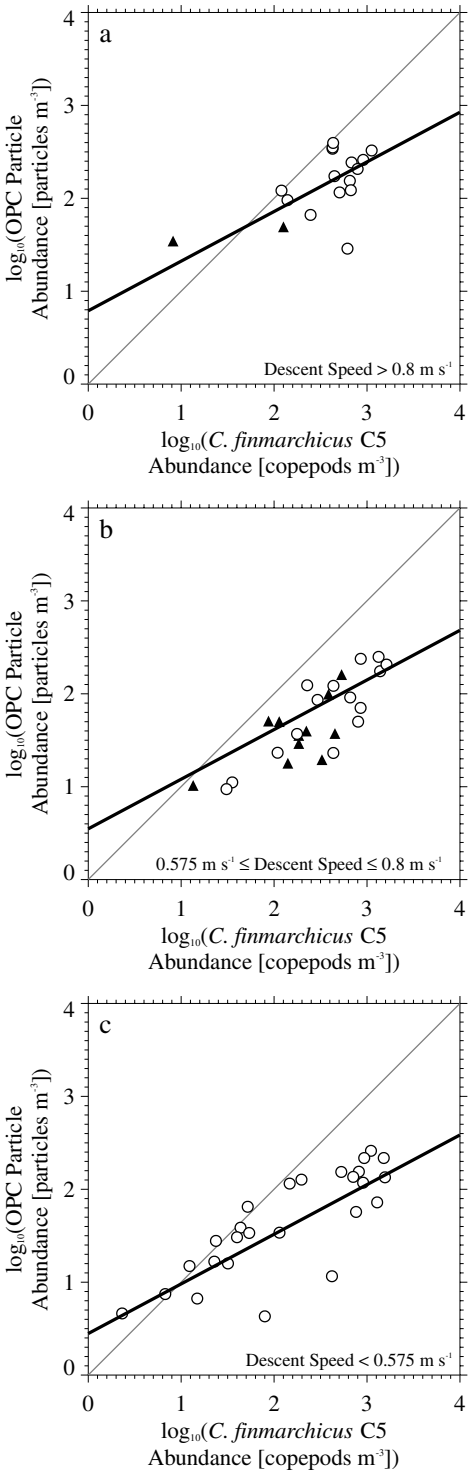

Fig. 6. Scatterplots of log-transformed *Calanus finmarchicus* C5 abundance and OPC particle abundance in the optimum size range for descent speeds (**a**) >0.8 m s^{-1} ('fast' AL0108 data), (**b**) between 0.575 and 0.8 m s^{-1} ('slow' AL0108 data) and (**c**) <0.575 m s^{-1} (DE9908). Data used to construct the final regression model (Table III) are shown as open circles. Lines indicate the final model corresponding to average descent speeds of (**a**) 0.94 m s^{-1}, (**b**) 0.63 m s^{-1} and (**c**) 0.51 m s^{-1}. The independent DE0007 data are shown as black triangles.

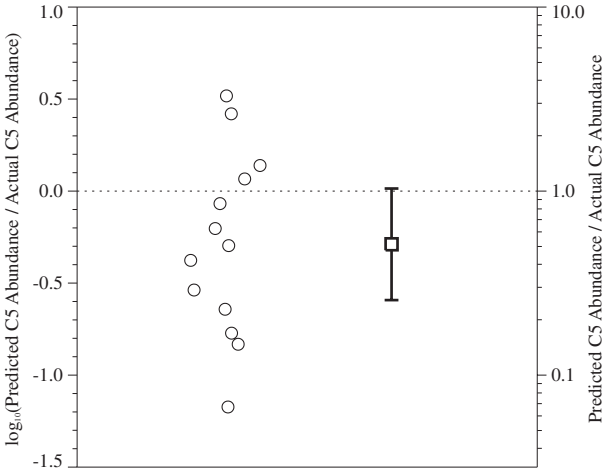

Fig. 7. Ratio of predicted to actual *C. finmarchicus* C5 net abundance for DE0007 data (circles) and the mean of the log-transformed ratio (square) with a 95% confidence interval (error bars).

only exceeded that of *C. finmarchicus* C5 on one occasion. Since smaller particles are more abundant than larger particles in general, the smaller half of the *C. finmarchicus* C5 size distribution is more likely to be obscured by either smaller copepods or detrital particles. In contrast, the larger half of this modal size distribution is infrequently obscured by less abundant, larger copepods or detrital material.

Avoidance of the OPC tunnel opening by *C. finmarchicus* C5 was inferred from the significantly higher particle abundances observed when descent speed was increased. This conclusion is also based on the observations of Miller and colleagues (Miller *et al.*, 1991) that resting *C. finmarchicus* C5 in this region are still responsive and capable of a strong escape reaction. The magnitude of this effect may be substantial. For the 0.30 m s^{-1} average increase in descent speeds between the 'fast' and 'slow' AL0108 data, median OPC particle abundance increased by a factor of 2.31 (95% CI: 1.45–3.66). For the same 0.30 m s^{-1} increase in descent speed, the analysis of the paired OPC casts yielded a lower estimate of the factor increase in median OPC particle abundance: 1.33 (95% CI: 1.16–1.53). Avoidance is a function of the size of the sampling aperture and the reaction time and escape velocity of the zooplankton (Barkley, 1964, 1972). The reaction time, in turn, is a function of the distance at which the animal can detect the sampler and the speed of the sampler. Although the sampling aperture and tow speed of an OPC can be held constant across applications, differences in the structure of the vehicle carrying the OPC can alter the pressure wave in front of the sampler and hence, the distance at which zooplankton can detect the oncoming sampler. Therefore, the estimates of the magnitude of avoidance

determined in this study are probably not directly applicable to other vehicles. However, the cage used in the present study was designed to reduce the pressure wave impacting the volume of water immediately in front of the OPC so avoidance was probably minimized. For larger vehicles or vehicles with obstructions near the OPC, the effect of avoidance on OPC particle abundances will probably be worse.

The final model predicted median *C. finmarchicus* C5 abundances from the DE0007 data that were too low by a factor of nearly 2. Most of the predictions (7 of 13) were within a factor of 3, while four of the predictions were gross underestimates between a factor of 4.4 and 14.9 too low. Unreasonably low OPC particle abundances were also observed on two occasions during DE9908 (Figure 4a). Underestimation of this type suggests that the single OPC casts accompanying each of these bongo tows did not sample the same population of *C. finmarchicus* C5 as did the net (i.e. the net sampled a patch of copepods while the OPC missed the patch). In a spatially heterogeneous environment, this would certainly be expected to happen occasionally. In fact, given this confounding by spatial heterogeneity and the differences in sampling methodology between the nets and the OPC, the correlations between the particle abundance and net-derived *C. finmarchicus* C5 abundance were remarkably high. Compared with the OPC, the nets integrated over a much larger horizontal spatial scale (hundreds of meters for towed nets versus discrete OPC vertical profiles), sampled a much larger volume of sea water (average net:OPC ratio of volume sampled was 300:1), probably experienced less avoidance (due to the larger sample aperture) and destroyed detrital particles that were counted by the OPC. Despite these significant differences, the coefficients of determination (r^2) were 0.655, 0.726 and 0.684 for the DE9908 data (Figure 4a), 'slow' AL0108 data (Figure 4b) and the final multiple linear regression model (Figure 6, Table III), respectively. When the two cases with unreasonably low OPC particle abundances are removed from the DE9908 data (Figure 4a), the agreement between the OPC and net abundances becomes much better ($r^2 = 0.840$). These coefficients of determination exceed those obtained by Heath and co-workers (Heath *et al.*, 1999) from samples and measurements collected in the Faroe–Shetland Channel between 500 and 1000 m with a side-by-side mounted plankton net and OPC.

Using a similar regression procedure, Heath and colleagues (Heath *et al.*, 1999) obtained maximum correlations in size ranges that nearly encompass the complete laboratory-derived *C. finmarchicus* C5 size distribution (0.90–1.70 mm in January, 1.02–1.74 mm in March). The abundance of both *C. finmarchicus* C4 and C5 were included in their analysis, but C5 dominated in both months. Heath and colleagues (Heath *et al.*, 1999) reported that their OPC sampled volumes between 0.25 and 0.5 m^3 during a single 60 s integration interval, which corresponds to tow speeds between 0.83 and 1.67 m s^{-1}. At the average descent speed used during the 'fast' AL0108 casts (0.94 m s^{-1}), the final model determined in this study predicts lower OPC particle abundances than those of Heath and colleagues for similar net abundances of *C. finmarchicus* C5 (Figure 8). Recall, however, that *C. finmarchicus* C5 was best detected in the larger half of its size distribution. Therefore, the final regression equation only models roughly half of the OPC particle abundance contributed by *C. finmarchicus* C5. The contribution of the smaller half of the size distribution can be taken into account simply by doubling the particle abundance obtained from the model. The resulting regression equation is now directly comparable to the Heath regression (Heath *et al.*, 1999) and there is excellent agreement between the two (Figure 8). In fact, no evidence was found to suggest that the regression coefficient for the net abundance of *C. finmarchicus* C5 (Table III) was different from the January (H_0: $\beta_1 = 0.492$, $P = 0.50$) or March (H_0: $\beta_1 = 0.461$, $P = 0.25$) slopes of the Heath regressions (Heath *et al.*, 1999). Because the results of these two studies are

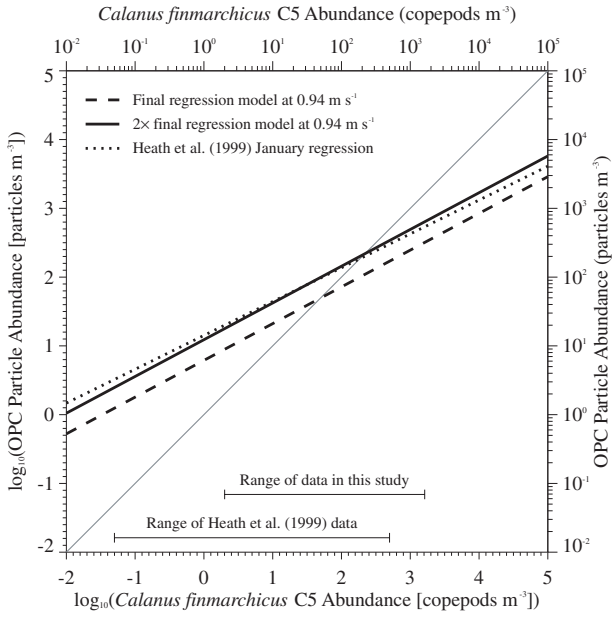

Fig. 8. Final multiple linear regression model (Table III) for a descent speed of 0.94 m s^{-1} (dashed line), the final model at 0.94 m s^{-1} with particle abundances doubled (solid line) and the January regression of Heath and colleagues (Heath *et al.*, 1999) (dotted line). The ranges of net-derived *C. finmarchicus* C5 abundances used in each study are shown. Note that only 4% of the samples from Heath and colleagues (Heath *et al.*, 1999) had combined *C. finmarchicus* C4 and C5 abundances >100 copepods m^{-3} whereas 74% of the samples in the present study had *C. finmarchicus* C5 abundances >100 copepods m^{-3}.

consistent, it seems reasonable to conclude that the regression lines in Figure 8 represent the true response of the OPC to varying abundances of *C. finmarchicus* C5 over nearly five orders of magnitude.

Calanus finmarchicus C5 abundance can be estimated in future studies from the OPC-derived abundance of particles between 1.5 and 2.0 mm using equation (6) and the coefficients in Table III. Since the OPC particle abundances used to determine these coefficients were between 4 and 395 particles m^{-3}, *C. finmarchicus* C5 abundances should only be prudently estimated with equation (6) when OPC particle abundances are in this same range. These particle abundances were determined over very coarse depth strata to be comparable to the *C. finmarchicus* C5 abundances from the corresponding net tows. The OPC, of course, has the capability to provide much finer-scale abundance and distribution information, but calibrating higher particle abundances sometimes found in narrower depth strata is difficult. Near right whales, peak abundances in 5 m depth strata typically exceed 395 particles m^{-3} and can range as high as 1100 particles m^{-3}. Estimating abundances of *C. finmarchicus* C5 using these OPC data requires extrapolation from the calibration equation. The results presented here indicate that the regressions of Heath and colleagues (Heath *et al.*, 1999) could be successfully extrapolated to higher concentrations, which provides some hope, yet no evidence, that these same regressions may apply to *C. finmarchicus* C5 abundances between 1000 and 10 000 copepods m^{-3} or higher.

At higher concentrations, coincidence counts (Herman, 1988) may occur if the concentration of smaller sized particles is also high. Coincidence would reduce the number of particles detected in the 1.5–2.0 mm size range and result in underestimation of the *C. finmarchicus* C5 abundance by the calibration equation. For OPC casts associated with net tows having *C. finmarchicus* C5 abundances >1000 copepods m^{-3}, the total time spent detecting particles (i.e. the total time particles spent traversing the 4 mm wide light beam plus a 4 ms per particle electronics reset time) during each 0.5 s interval of a downcast was rarely >0.25 s. If coincidence counting were frequent, this total processing time would be much closer to 0.5 s. Even near right whales, where discrete layers of particles in the optimum size range can exceed abundances of 1000 particles m^{-3}, total processing time remains below 0.25 s. These results suggest that coincident counting occurs infrequently and it will not affect estimates from the calibration equation for the observed range of OPC particle abundances. Fleminger and Clutter (Fleminger and Clutter, 1965) suggest that avoidance may decrease at higher concentrations, which would result in overestimation of the *C. finmarchicus* C5 abundance by the calibration equation. A test of an additional interaction term [$\log_{10}(NET) \times SPEED$] in the model described by equation (3), however, provided no evidence that the effect of avoidance on the OPC particle abundance varied with *C. finmarchicus* C5 abundance over concentrations between 31 and 1621 copepods m^{-3} ($P = 0.31$). With no evidence of either persistent coincident counting or decreased avoidance at higher concentrations and with appropriate caution, extrapolation of the calibration equation to predict *C. finmarchicus* C5 concentrations from higher OPC particle abundances seems feasible.

Because the calibration equation (equation 6) was developed from comparisons with nets, it is designed to predict *C. finmarchicus* C5 abundances that are equivalent to abundances that could be obtained with nets. None of the issues surrounding net sampling (e.g. net avoidance, extrusion, clogging) have been taken into account in this model, however these problems were not expected to contribute large errors in abundance estimates because the appropriate nets and mesh sizes to sample adequately *C. finmarchicus* C5 were used in this study (Anderson and Warren, 1991; Nichols and Thompson, 1991). Verification of the accuracy of this calibration model in other environments with similar net sampling is therefore possible. In fact, validation of this model with net sampling prior to use is essential, since the model is predicated on *C. finmarchicus* C5 dominance in the 1.5–2.0 mm particle size range. In environments where this is not the case, the model is expected to perform poorly. However, given the dominance of *C. finmarchicus* in many North Atlantic regions and the current questions about the ecology of the fifth copepodite resting stock, I anticipate that the OPC and this calibration equation will serve as useful tools in future *C. finmarchicus* research.

ACKNOWLEDGEMENTS

I am indebted to many people for contributing equipment, laboratory space and expertise: Shailer Cummings and Peter Ortner for the OPC used during 1999, Bruce Mate for the OPC used during 2000 and 2001, Jerry Prezioso for the bongo equipment, Bob Campbell and Greg Teegarden for use of and assistance with the University of Rhode Island MOCNESS, Rick Trask for assistance with the OPC/CTD cage construction and Charlie Miller and Carin Ashjian for laboratory facilities. I am also grateful for the support and able assistance of the chief scientists on all of the cruises, Tim Cole and Phil Clapham, and the master, officers and crew of NOAA Ships *Delaware II* and *Albatross IV*. Helpful criticisms of earlier drafts were provided by Charlie Miller and Are Edvardsen. This work was supported by the National

Marine Fisheries Service, Office of Naval Research, Oregon State University Marine Mammal Endowment and the Space Grant and Earth System Science fellowship programs of the National Aeronautics and Space Administration.

REFERENCES

Anderson, J. T. and Warren, W. G. (1991) Comparison of catch rates among small and large bongo samplers for *Calanus finmarchicus* copepodite stages. *Can. J. Fish. Aquat. Sci.*, **48**, 303–308.

Barkley, R. A. (1964) The theoretical effectiveness of towed-net samplers as related to sampler size and to swimming speed of organisms. *J. Cons. Perm. Int. Explor. Mer.*, **29**, 146–157.

Barkley, R. A. (1972) Selectivity of towed-net samplers. *Fish. Bull.*, **70**, 799–820.

Beardsley, R. C., Epstein, A. W., Chen, C., Wishner, K. F., Macaulay, M. C. and Kenney, R. D. (1996) Spatial variability in zooplankton abundance near feeding right whales in the Great South Channel. *Deep-Sea Res. II*, **43**, 1601–1625.

Checkley, D. M. Jr., Ortner, P. B., Settle, L. R. and Cummings, S. R. (1997) A continuous, underway fish egg sampler. *Fish. Oceanogr.*, **6**, 58–73.

Davis, C. S., Gallager, S. M., Berman, M. S., Haury, L. R. and Strickler, J. R. (1992) The video plankton recorder (VPR): design and initial results. *Arch. Hydrobiol. Beih. Ergebn. Limnol.*, **36**, 67–81.

Davis, C. S., Gallager, S. M., Marra, M. and Stewart, W. K. (1996) Rapid visualization of plankton abundance and taxonomic composition using the Video Plankton Recorder. *Deep-Sea Res. II*, **43**, 1947–1970.

Edvardsen, A. (2002) Determining zooplankton ESD signatures using an *in situ* OPC in the laboratory. In Zhou, M. and Tande, K. (eds), *Optical Plankton Counter Workshop*. GLOBEC Report 17., GLOBEC International Project Office, Plymouth, UK, pp. 16–21.

Fleminger, A. and Clutter, R. I. (1965) Avoidance of towed nets by zooplankton. *Limnol. Oceanogr.*, **10**, 96–104.

Focal Technologies (1999) *Optical Plankton Counter Users's Guide*. Focal Technologies, Inc., Dartmouth, NS, Canada.

Grant, S., Ward, P., Murphy, E., Bone, D. and Abbott, S. (2000) Field comparison of an LHPR net sampling system and an optical plankton counter (OPC) in the Southern Ocean. *J. Plankton Res.*, **22**, 619–638.

Halliday, N. C., Coombs, S. H. and Smith, C. (2001) A comparison of LHPR and OPC data from vertical distribution sampling of zooplankton in a Norwegian fjord. *Sarsia*, **86**, 87–99.

Heath, M. R. (1995) Size spectrum dynamics and planktonic ecosystem of Loch Linnhe. *ICES J. Mar. Sci.*, **52**, 627–642.

Heath, M. R., Dunn, J., Fraser, J. G., Hay, S. J. and Madden, H. (1999) Field calibration of the optical plankton counter with respect to *Calanus finmarchicus*. *Fish. Oceanogr.*, **8** (suppl. 1), 13–24.

Herman, A. W. (1988) Simultaneous measurement of zooplankton and light attenuance with a new optical plankton counter. *Cont. Shelf Res.*, **8**, 205–221.

Herman, A. W. (1992) Design and calibration of a new optical plankton counter capable of sizing small zooplankton. *Deep-Sea Res.*, **39**, 395–415.

Herman, A. W., Sameoto, D. D., Shunnian, C., Mitchell, M. R., Petrie, B. and Cochrane, N. (1991) Sources of zooplankton on the Nova Scotia Shelf and their aggregations within deep-shelf basins. *Cont. Shelf Res.*, **11**, 211–238.

Herman, A. W., Cochrane, N. A. and Sameoto, D. D. (1993) Detection and abundance estimation of euphausiids using an optical plankton counter. *Mar. Ecol. Prog. Ser.*, **94**, 165–173.

Hirche, H.-J. (1996) Diapause in the marine copepod, *Calanus finmarchicus* – a review. *Ophelia*, **44**, 129–143.

Holliday, D. V. and Pieper, R. E. (1995) Bioacoustical oceanography at high frequencies. *ICES J. Mar. Sci.*, **52**, 279–296.

Huntley, M. E., Zhou, M. and Nordhausen, W. (1995) Mesoscale distribution of zooplankton in the California Current in late spring, observed by Optical Plankton Counter. *J. Mar. Res.*, **53**, 647–674.

Kenney, R. D., Hyman, M. A. M., Owen, R. E., Scott, G. P. and Winn, H. E. (1986) Estimation of prey densities required by western North Atlantic right whales. *Mar. Mamm. Sci.*, **2**, 1–13.

Mayo, C. A. and Marx, M. K. (1990) Surface foraging behavior of the North Atlantic right whale, *Eubalaena glacialis*, and associated zooplankton characteristics. *Can. J. Zool.*, **68**, 2214–2220.

Miller, C. B., Cowles, T. J., Wiebe, P. H., Copley, N. J. and Grigg, H. (1991) Phenology in *Calanus finmarchicus*; hypotheses about control mechanisms. *Mar. Ecol. Prog. Ser.*, **72**, 79–91.

Murison, L. D. and Gaskin, D. E. (1989) The distribution of right whales and zooplankton in the Bay of Fundy, Canada. *Can. J. Zool.*, **67**, 1411–1420.

Nautical Software (1996) *Tides and Currents, version 2.0 Users Guide*, 3rd edn. Nautical Software, Inc., Beaverton, OR, USA.

Nichols, J. H. and Thompson, A. B. (1991) Mesh selection of copepodite and nauplius stages of four calanoid copepod species. *J. Plankton Res.*, **13**, 661–671.

Osgood, K. E. and Checkley, D. M. Jr. (1997) Observations of deep aggregations of *Calanus pacificus* in the Santa Barbara Basin. *Limnol. Oceanogr.*, **42**, 997–1001.

Ramsey, F. L. and Schafer, D. W. (1997) *The Statistical Sleuth: a Course in Methods of Data Analysis*. Duxbury Press, Belmont, CA.

Sameoto, D. D. and Herman, A. W. (1990) Life cycle and distribution of *Calanus finmarchicus* in deep basins on the Nova Scotia shelf and seasonal changes in *Calanus* spp. *Mar. Ecol. Prog. Ser.*, **66**, 225–237.

Sameoto, D., Cochrane, N. and Herman, A. (1993) Convergence of acoustic, optical and net-catch estimates of euphausiid abundance: use of artificial light to reduce net avoidance. *Can. J. Fish. Aquat. Sci.*, **50**, 334–346.

Sprules, W. G., Jin, E. H., Herman, A. W. and Stockwell, J. D. (1998) Calibration of an optical plankton counter for use in fresh water. *Limnol. Oceanogr.*, **43**, 726–733.

Stockwell, J. D. and Sprules, W. G. (1995) Spatial and temporal patterns of zooplankton biomass in Lake Erie. *ICES J. Mar. Sci.*, **52**, 557–564.

Stone, G. S., Kraus, S. D., Prescott, J. H. and Hazard, K. W. (1988) Significant aggregations of the endangered right whale, *Eubalaena glacialis*, on the continental shelf of Nova Scotia. *Can. Field Nat.*, **102**, 471–474.

Tande, K. and Miller, C. B. (1996) Preface to: Trans-Atlantic Study of *Calanus finmarchicus*, Proceedings of a Workshop. *Ophelia*, **44**, i–ii.

Wiebe, P. H., Burt, K. H., Boyd, S. H. and Morton, A. W. (1976) A multiple opening/closing net and environmental sensing system for sampling zooplankton. *J. Mar. Res.*, **34**, 313–325.

Wiebe, P. H., Morton, A. W., Bradley, A. M., Backus, R. H., Craddock, J. E., Barber, V., Cowles, T. J. and Flierl, G. R. (1985) New

developments in the MOCNESS, an apparatus for sampling zooplankton and micronekton. *Mar. Biol.*, **87**, 313–323.

Wiebe, P. H., Beardsley, R. C., Bucklin, A. and Mountain, D. G. (2001) Coupled biological and physical studies of plankton populations in the Georges Bank region and related North Atlantic GLOBEC study sites. *Deep-Sea Res. II*, **48**, 1–2.

Wieland, K., Petersen, D. and Schnack, D. (1997) Estimates of zooplankton abundance and size distribution with the optical plankton counter (OPC). *Arch. Fish. Mar. Res.*, **45**, 271–280.

Wishner, K., Durbin, E., Durbin, A., Macaulay, M., Winn, H. and Kenney, R. (1988) Copepod patches and right whales in the Great South Channel off New England. *Bull. Mar. Sci.*, **43**, 825–844.

Wishner, K. F., Schoenherr, J. R., Beardsley, R. and Chen, C. (1995) Abundance, distribution and population structure of the copepod *Calanus finmarchicus* in a springtime right whale feeding area in the southwestern Gulf of Maine. *Cont. Shelf Res.*, **15**, 475–507.

Woodd-Walker, R. S., Gallienne, C. P. and Robins, D. B. (2000) A test model for optical plankton counter (OPC) coincidence and a comparison of OPC-derived and conventional measures of plankton abundance. *J. Plankton Res.*, **22**, 473–483.

Woodley, T. H. and Gaskin, D. E. (1996) Environmental characteristics of North Atlantic right and fin whale habitat in the lower Bay of Fundy, Canada. *Can. J. Zool.*, **74**, 75–84.

Zar, J. H. (1999) *Biostatistical Analysis*, 4th edn. Prentice Hall, Upper Saddle River, NJ.

Zhang, X., Roman, M., Sanford, A., Adolf, H., Lascara, C. and Burgett, R. (2000) Can an optical plankton counter produce reasonable estimates of zooplankton abundance and biovolume in water with high detritus? *J. Plankton Res.*, **22**, 137–150.

Received on December 12, 2002; accepted on March 25, 2003